ACS APPLIED MATERIALS & INTERFACES

Research Article

www.acsami.org

Development of a Templated Approach to Fabricate Diamond Patterns on Various Substrates

Olga Shimoni,*[,†,§] Jiri Cervenka,[†,⊥] Timothy J. Karle,[†] Kate Fox,[†] Brant C. Gibson,[†,‡] Snjezana Tomljenovic-Hanic,[†] Andrew D. Greentree,[‡] and Steven Prawer[†]

[†]School of Physics, The University of Melbourne, Parkville, Victoria 3010, Australia

[‡]Chemical and Quantum Physics, School of Applied Sciences, RMIT University, Melbourne, Victoria 3001, Australia

Supporting Information

ABSTRACT: We demonstrate a robust templated approach to pattern thin films of chemical vapor deposited nanocrystalline diamond grown from monodispersed nanodiamond (mdND) seeds. The method works on a range of substrates, and we herein demonstrate the method using silicon, aluminum nitride (AlN), and sapphire substrates. Patterns are defined using photo- and e-beam lithography, which are seeded with mdND colloids and subsequently introduced into microwave assisted chemical vapor deposition reactor to grow patterned nanocrystalline diamond films. In this study, we investigate various factors that affect the selective seeding of different substrates to create high quality diamond thin films, including mdND surface termination, zeta potential, surface treatment, and plasma cleaning. Although the electrostatic interaction between mdND colloids and substrates is the main process driving adherence, we found that chemical reaction (esterification) or hydrogen bonding can potentially dominate the seeding process. Leveraging the knowledge on these different interactions, we optimize fabrication protocols to eliminate unwanted diamond nucleation outside the patterned areas. Furthermore, we have achieved the deposition of patterned diamond films and arrays over a range of feature sizes. This study contributes to a comprehensive understanding of the mdND−substrate interaction that will enable the fabrication of integrated nanocrystalline diamond thin films for microelectronics, sensors, and tissue culturing applications.

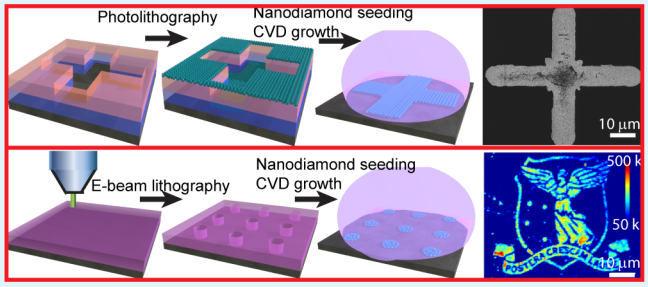

KEYWORDS: *nanodiamonds, microwave-assisted chemical vapor deposition (CVD), patterning, photolithography, substrate, aluminum nitride, sapphire*

INTRODUCTION

The excellent properties[1−3] of nanocrystalline diamond (NCD) thin films produced by chemical vapor deposition (CVD) have attracted interest due to their promising applications in diverse areas, such as micro-electro-mechanical systems (MEMS),[4,5] substrates for heat dissipation,[6−8] and substrates for cell growth in tissue culturing.[9,10] In addition, diamond thin films are considered for solid-state optical approaches to quantum information processing, as they possess a wide transparency window in the visible regime, have a high thermal conductivity, and most critically, host a large number of high dipole-moment color centers, such as the nitrogen-vacancy (NV), silicon-vacancy (SiV), and other centers.[11,12]

Traditionally, to initiate a diamond CVD growth on non-diamond surfaces, the substrates have been immersed into a suspension of detonation nanodiamonds (NDs), which consist of various sizes of agglomerates and agglutinates (slurry).[13,14] More recently, monodispersed nanodiamond (mdND) colloids have been used as a primer for a high-density diamond seeding and nucleation to grow nanocrystalline films on non-diamond substrates.[15,16] Typically, in this process, silicon or silica substrates are seeded using mdND colloid suspensions utilizing electrostatic interaction between the nanoparticles and the substrate, followed by growth in a CVD reactor.[17,18] The use of mdND colloids for seeding is important, as it promotes a high nucleation density. In addition, because the seeding layer is based on mdNDs, it creates a uniform, high-density layer without agglomeration, which leads to a more homogeneous growth of the NCD film.

Although seeding from a ND suspension is suitable for a large-scale diamond film growth, it is not ideal for high precision applications, where micrometer and submicrometer resolution is required. Examples of applications that require such high precision specific growth would include field effect transistors, sensor electrodes, and nano and micro electro-mechanical systems devices. When patterned diamond thin films are fabricated, it is common for CVD grown films to be etched using reactive ion etching technology,[19] or a micro-

Received: March 19, 2014
Accepted: May 12, 2014
Published: May 30, 2014

   dx.doi.org/10.1021/am5016556 | ACS Appl. Mater. Interfaces 2014, 6, 8894−8902

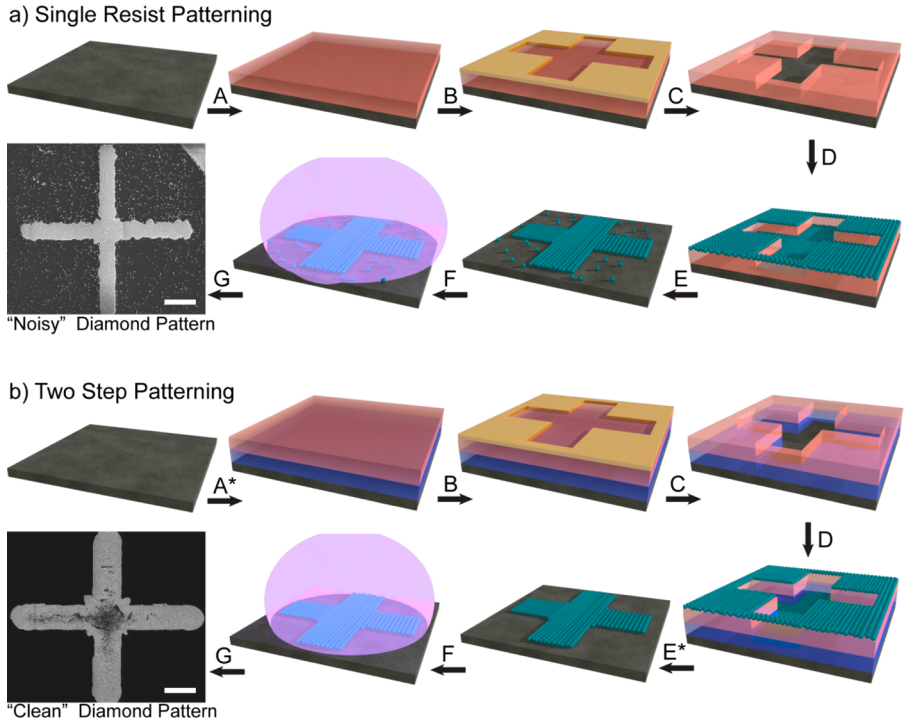

Figure 1. (a) Schematic representation of the single photoresist lithography to pattern diamond thin film on silicon substrate. A thin layer of positive photoresist (red) is spun on the surface of substrate and cured (A), covered with a chrome mask (gold), and exposed to a broadband UV light (B). After exposure to a UV light, the photoresist is rinsed in a developer to create openings (C). Following that, the substrate with a developed photoresist is immersed into mdND colloidal suspension, where mdNDs homogeneously cover (green) the whole surface (D). Subsequently, photoresist is removed using acetone (E), and the substrate with remaining mdND seeds is inserted into MWCVD reactor for diamond growth (F). This approach results in a "noisy" diamond pattern on silicon (G) as determined by SEM micrograph. (b) Schematic representation of the double photoresist approach to pattern diamond thin film on silicon substrate. The approach is similar to the above method, except that here we use a lift-off resist (blue) in addition to the standard photoresist (A*). Processes B, C, and D are identical to those described in panel (a). The removal of photoresist (E*) is a two-step process, where the first photoresist is removed using acetone (similar to process E) and the lift-off resist is removed by means of developer. Accordingly, the pattern is inserted into CVD reactor for a diamond growth (F). This approach results in a "clean" diamond pattern (G) as determined by SEM micrograph. Scale bars are 10 μm.

machining method, such as laser ablation[20] (top-down approach). Top-down processing is effective, but can be a costly and resource demanding technique, particularly for high aspect ratio structures. In addition, the "top-down processing" causes instability in optical color centers located close to the surface.[21,22]

Alternatively, we demonstrate a general method to fabricate patterned NCD thin films with micrometer and submicrometer resolution using a combination of photolithography and colloid seeding from the mdND suspensions. The use of mdND is essential to obtain the high-quality diamond films, and therefore careful preparation of the as-received detonation ND is required. Following the annealing approach developed by our and other groups,[23,24] aqueous mdND colloidal suspensions were prepared using thermally treated detonation ND powder. Specifically, we de-agglomerate detonation NDs by annealing in oxygen or hydrogen gases followed by centrifugation, which led to negatively and positively charged suspensions, respectively. Obtaining mdNDs with the opposite charges is beneficial for a realization of electrostatic interaction between the mdNDs and various substrates.

Importantly, our results show that to realize high quality patterns, it is essential to control multiple factors, including ND termination, substrate charge and reactivity, photoresist, and developer. Accordingly, we reveal that although the electrostatic interactions are the main driving force for interaction between the substrates and mdND suspensions, there are other forces and factors to be considered. Therefore, in this work, we develop recipes for the creation of high-quality NCD patterns on silicon, aluminum nitride (AlN), and sapphire by investigating various mdNDs−substrate interactions. We performed a patterned growth of diamond on sapphire that extends this research into applications, such as nitrogen-vacancy-based quantum optics, where it is desirable to grow ND arrays on silicon-deficient substrates to avoid the incorporation of silicon-vacancy centers.[25] Furthermore, we demonstrate an increase in the resolution of the diamond patterns using a combination of e-beam lithography and the mdND seeding procedures. We show that a deposition of fewer than 5 NDs is achievable within the 100 nm E-beam aperture size in a patterned manner over a range of feature sizes (from micrometer to submicrometer).

EXPERIMENTAL SECTION

Materials. The *p*-type doped Si wafers (100), positive photoresist AZ1614H, lift-off resist LOR 5B, and developer AZ826MIF were purchased from M.M.R.C. Pty Ltd. For the high-resolution patterning, *n*-type doped Si wafers were purchased from the same source, coated with poly(methyl methacrylate) A2 (PMMA A2) in anisole solvent, and a mix of MIBK:IPA (1:3) developer was used. AlN was purchased from Kyma Technologies, Inc. as a 200 nm thin film with C-plane orientation grown on Si (111). The sapphire substrate was obtained from GT Advanced Technologies as single side polished, light emitting diode grade substrate with orientation (0001). Detonation NDs were

dx.doi.org/10.1021/am5016556 | ACS Appl. Mater. Interfaces 2014, 6, 8894−8902

obtained from PlasmaChem GmbH as a ND (>97%) powder grade G01. All solvents were used as received.

Methods. *Single Photoresist Lithography.* Cleaved substrates (Si with native oxide layer, AlN on silicon or sapphire) with surface area of approximately 0.5 cm^2 were cleaned in three organic solvents (acetone, methanol, isopropyl alcohol) for 5 min using an ultrasonic bath, rinsed in deionized water (DI), and dried under a steady flow of high-purity nitrogen gas. A subset of the samples was subsequently treated in an oxygen plasma cleaner (25 % oxygen in argon) for 2 min. A thin layer (1.4 μm) of the AZ1514H resist was spin-coated (Speedline Coating Systems P6708) on a chosen substrate (4000 rpm for 1 min) and cured for 1 min at 100 °C (Figure 1a, process A). A chromium on quartz mask was brought into contact with the samples using a Quintel Mask Aligner, and the photoresist was exposed to a broadband ultraviolet (UV) mercury lamp for 15 s (Figure 1a, process B). Exposed areas were developed with AZ826MIF for 25 s (Figure 1a, process C). To eliminate a residual photoresist layer in the openings, selected samples were additionally treated in an oxygen plasma cleaner for 0.5−1 min.

Two-Step Photoresist Lithography. Cleaved samples were cleaned as described above. LOR 5B was spin-coated on the substrates (4000 rpm for 1 min) and cured for 1 min at 190 °C. An additional layer of AZ1514H was spun on top of LOR 5B (4000 rpm for 1 min) and further cured for 1 min at 100 °C (Figure 1b, process A*). A quartz mask was used with the mask aligner, and both resists were exposed to a broadband UV light for 15 s (Figure 1b, process B). Exposed areas were developed using AZ826MIF for 25 s, rinsed in DI water (Figure 1b, process C).

E-Beam Lithography. The *n*-type doped Si substrates measuring approximately 0.5 cm^2 in size were cleaned in two organic solvents (acetone, isopropyl alcohol) for 5 min using an ultrasonic bath, rinsed in deionized water (DI), and dried under a steady flow of high-purity nitrogen gas. PMMA A2 was applied and spun at 5000 rpm for 1 min, forming a 100 nm thick resist layer. Patterns were exposed using a 30 kV electron beam focused to a <100 nm size spot. Either 200 nm diameter circular patterns were raster scanned or single dot points were exposed using a Raith pattern generator at a dose of 300 $\mu A/cm^2$. The patterns were developed in MIBK:IPA (1:3) for 30 s and then rinsed in DI water before being dried under a steady flow of high-purity nitrogen gas.

Colloid Seeding and Patterning. Monodispersed aqueous ND colloidal solutions were prepared using thermally treated detonation ND powder. Annealing of the detonation NDs was performed individually in two gaseous environments: in oxygen gas (purity 99.999%) at 400 °C for 4 h, and in forming gas (14% hydrogen in argon) at 800 °C for 17 h. The annealed powders were dispersed in Milli-Q water (Millipore RiOs/Origin system, resistance >18 MΩ) as 1.5 mg mL^{-1} dispersions, ultrasonicated for 0.5 h, and centrifuged for 6 h at 20000*g* to obtain monodispersed diamond suspensions (supernatants) with an average diameter particle size of 4−5 nm. Dispersions of NDs after annealing in hydrogen gas exhibited a positive charge and those annealed in oxygen were negatively charged (Table 1).

Once the patterned substrates were developed, they were immersed into mdND colloid suspensions (annealed in hydrogen or oxygen environment) for 5 min in an ultrasonic bath, then rinsed in DI water, and dried in a nitrogen gas flow (Figure 1a, process D). Once the samples were seeded with mdND, the photoresist was stripped from the samples with acetone (both AZ1514H and PMMA) (Figure 1a, process E). When samples were prepared using the two-step photolithography procedure, the photoresist was removed with acetone, while the LORB was removed with AZ826MIF developer (Figure 1b, process E*). Following this, the samples were rinsed in DI water and dried with a nitrogen gas flow.

Table 1. Zeta Potential and Sizes of the Different ND Colloidal Suspensions[a]

	zeta potential, mV	size distribution, nm
ND as received	−31.9 ± 5.4	197.7 ± 69.0
ND after annealing in O_2	−50.9 ± 5.5	3.8 ± 1.2
ND after annealing in H_2	+63 ± 20.4	21.4 ± 11.0

[a]The values of zeta potential and size distribution of ND after annealing and centrifugation.

Diamond Powders Characterization. Fourier transform infrared spectroscopy (FTIR) spectra of the treated ND powders were acquired using a FTIR Bruker Tensor 27 spectrometer with a high sensitivity DLaTGS detector with a KBr window at a resolution of 4 cm^{-1} and 16 scans. Samples were prepared as KBr pellets containing 2 mg of ND powder ground thoroughly with dry 100 mg of KBr powder (FTIR grade) and pressed into a 7 mm disk using the Specac 10 ton hydraulic press. ND size and zeta potential in the colloidal dispersions were characterized using a Malvern Zetasizer Nano ZS fitted with a 633 nm laser.

Nanocrystalline Diamond (NCD) Film Growth. To obtain high-quality NCD thin films, all the seeded samples were placed into microwave-assisted chemical vapor deposition (MWCVD) reactor (Cyrannus system, Iplas GmbH). All diamond films were grown using 2000 W of input power, and a chamber pressure of 80 Torr with total gas flow of 760 sccm hydrogen/methane mixture (1.3% methane in hydrogen) for 20 min (Figure 1, process F). Using high hydrogen to methane gas ratio with high chamber pressure allows a growth of high quality diamond from diamond seeds, while suppressing the diamond nucleation from other sources.

NCD and Substrate Characterization. X-ray photoelectron spectroscopy (XPS) was performed to determine a surface quality of the used substrates. XPS analysis was carried out on a ThermoFisher K-Alpha XPS equipped with an Mg−Kα monochromated X-ray source at a power of 300 W, and the pressure in the analysis chamber was less than 1×10^{-8} mbar. The elemental composition of the samples was quantified from survey spectra with a pass energy of 200 eV, whereas high-resolution spectra from individual peaks were acquired at a pass energy of 50 eV with a step size of 0.1 eV. The spot size of analysis was 400 μm. Sample charging during analysis was compensated by the internal flood gun. The background carbon contamination of the XPS system is less than 1 at. %. Data was processed and evaluated using Casa XPS software.

Scanning electron microscopy (SEM) micrographs were obtained on a FEI Nova dual beam apparatus operating under accelerating voltage of 5 kV, current of 98 pA, and working distance of approximately 5 mm.

A logo of the University of Melbourne was patterned using an identical e-beam lithography technique. The logo includes submicrometer features and covered an area of approximately 50 × 50 μm. The logo was imaged in a confocal microscope, using a 532 nm pump laser and a 0.6 NA objective to excite and collect fluorescence from SiV^- color centers within the diamond lattice, whose zero phonon line emission wavelength exhibits a sharp peak at 738 nm.

RESULTS AND DISCUSSION

Nanodiamond Colloids. To achieve a homogeneous growth of the diamond film, it is necessary to obtain well-dispersed mdND suspensions. As-received detonation NDs have to be treated as they possess a large amount of aggregation (Table 1). There have been a large number of reports describing de-agglomeration of NDs, including acid−base treatment, annealing in various gas environments, and milling with beads.[26] Treating of ND powders at elevated temperatures within a particular gas provides a sustainable method to diminish agglomeration without the need of harsh chemicals or addition of metal contaminants. Additionally, NDs treated in a gaseous environment do not compromise their biocompatibility as there is no introduction of toxic or harsh chemicals.[26]

Annealing of NDs in oxygen environment (at 400 °C) introduces a high number of hydroxyl and carboxylic groups (Figure SI 1, Supporting Information) on the surface of

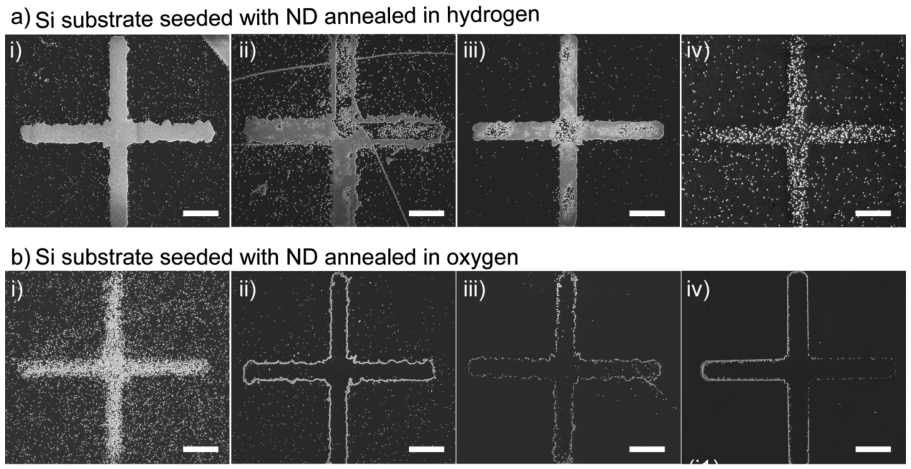

Figure 2. SEM images of the silicon substrates with fabricated diamond patterns prepared using single resist photolithography patterning approach and CVD growth. (a) Substrates were seeded using positively-charged mdNDs (annealed in hydrogen); (b) substrates were seeded with negatively-charged mdNDs (annealed in oxygen). (i) As-fabricated diamond pattern using processes A–F from Figure 1; (ii) substrate with a developed photoresist (after process C) was additionally treated in oxygen plasma cleaner for 30 sec; (iii) Si surface was treated in oxygen plasma cleaner before the photolithography process (before A) and after developing of photoresist (before process D); (iv) after photolithography and seeding procedures (before process F), the sample was exposed to a hydrogen plasma in the CVD chamber for few minutes prior to a diamond growth. Scale bars are 10 μm.

mdNDs, leading to negatively charged oxygen-terminated particles in a water suspension (Table 1). In the same manner, annealing diamond powders in a hydrogen environment (at 800 °C) terminates the surface of diamond with hydrogen groups that lead to the surface transfer doping phenomenon in water, resulting in a positive zeta potential (Table 1).[27,28] The surface charge of the diamond nanoparticles has been found to be crucial for the patterning of various surfaces through the colloidal seeding procedure.[29] Moreover, the size distribution of the mdND colloids is equally important as it assists in homogeneous diamond nucleation and growth, which is particularly important for nanocrystalline diamond films. Therefore, after annealing treatment and dispersion in water, ND suspensions have been further centrifuged to obtain stable monodispersed suspensions (Table 1). It is notable from Table 1 that the average size of the oxygen-treated mdNDs is smaller than the hydrogen-treated mdNDs, suggesting that oxygen etching of a graphitic part is more effective in breaking agglomerates. Hydrogen treatment reduces graphitic and other surface groups to produce hydrogenated NDs, but annealing in hydrogen is less effective in breaking agglomerates compared with oxygen. The more efficient hydrogen plasma-based technique was proposed by Girard and Arnault et al.,[30] although we have not evaluated their method with our processing.

Single Resist Patterning Method. Photolithography offers a relatively low-cost and easy way to create high resolution patterns on various surfaces using a photoresist (Figure 1a, A–C). Immersion of a fabricated pattern into an appropriate ND suspension leads a uniform surface coverage of NDs (Figure 1a, D). Following the photoresist removal, a thin diamond film is grown in the CVD that approximately conforms to the seeded area (Figure 1a, F). A scanning electron microscopy micrograph of a CVD-grown patterned NCD film on Si produced using photolithography technique and mdND seeding is shown in Figure 1a, G. It is noticeable that the cross pattern has rough edges and numerous diamonds can be found outside of the patterned regions.

As silicon wafers inherently possess a native silicon oxide layer, silicon substrates present a negative surface charge on their surfaces. Accordingly, based on the previous work of Hees et al.,[17] we expected that the electrostatic interaction plays a major role in the seeding of the substrates, where positively charged mdNDs are attracted to the negatively charged surface while the negatively charged are repulsed. However, our findings here show that other factors strongly influence the mdND-surface interaction and the precision and the density of the patterned NCD thin films. The diamond patterns have been nucleated not only using positively-charged mdNDs on silicon oxide layer (ND–substrate attraction, Figure 2a, i) but also using a negatively-charged mdND suspension (ND–substrate repulsion, Figure 2b, i). As expected, well-defined patterns have been formed using positively-charged mdND suspensions (Figure 2a, i) with some diamond nucleation outside the patterns. The nucleation outside of patterns occurred possibly because some mdNDs are attracted back to the surface during a photoresist removal in acetone.

Surprisingly, there are also defined patterns formed via seeding with negatively charged colloids (Figure 2b, i). During resist removal some of the particles could reattach back to the surface through hydrogen interaction or van der Waals forces. However, increased density of diamond seeding where the photoresist was developed most likely, due to the chemical reaction (esterification) happening between mdNDs and a remaining thin layer of the photoresist. Specifically, in this case, we used a positive photoresist that consists of novolac resin possessing hydroxyl groups (Scheme 1). The evidence of novolac presence was confirmed by X-ray photoelectron spectroscopy (XPS). The deconvolution of C 1s XPS of the used photoresist clearly shows this C–OH component (Figure 3 v). In addition, XPS also identifies a small amount of remaining photoresist on the surface of silicon after exposure to UV and removal with a developer. Furthermore, mdNDs with carboxylic acid groups dispersed in pure water present an acidic pH,[31] which contributes to the esterification reaction. Although the esterification reaction is a relatively slow process, ultrasonication during the seeding can provide the essential

Scheme 1. Schematic of the Esterification Reaction Happening between the Oxygen-Treated mdNDs with Carboxylic Acid Groups and the Remaining Layer of Photoresist Containing Novolac Polymer[a]

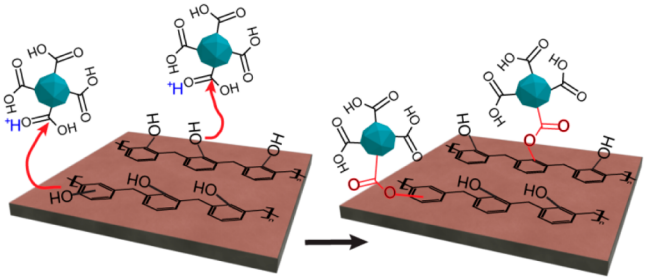

[a]Typically, during the esterification reaction, protons from the acidic environment interact with a carbonyl on the carboxylic acid and leave the carbonyl carbon with an electron deficiency. The electron pair on the hydroxyl is attracted to that carbon, while the proton from the hydroxyl attaches to the hydroxyl on the carboxylic group, leading to the water molecule as a good releasing group. One of the remaining protons returns back to the acid available in the solution, leading to carbonyl closure and eventually a formation of ester bond.

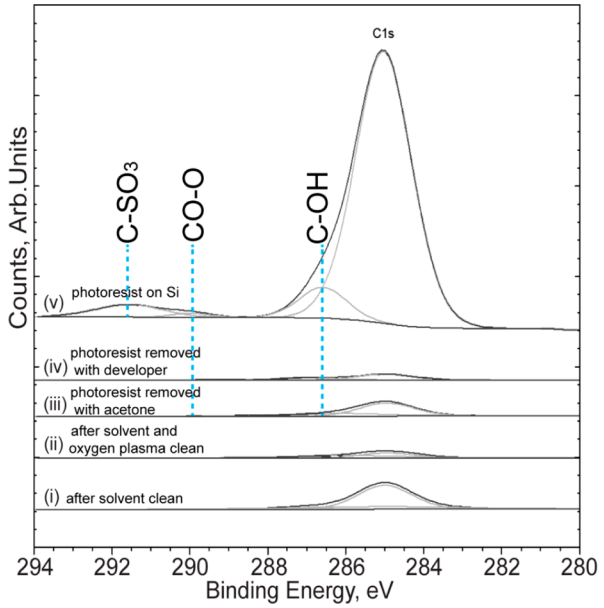

Figure 3. XPS spectra of the C 1s peak to determine the amount of the hydrocarbon that remains on silicon wafer before the diamond growth. Carbon peaks on the Si surface originate from solvent cleaning (i), solvents after oxygen/argon plasma cleaner (ii), photoresist removed with acetone (iii), photoresist removed with a developer (iv), and photoresist itself (v). Si after solvent cleaning and treating in oxygen plasma cleaner exhibits a negligible amount of carbon (ii). A similar result has been obtained with the surface, where the photoresist was exposed to UV light followed by removal with the developer, leading to only a small amount of the remaining photoresist (iv). On the other hand, the surface with the photoresist removed with acetone has been left with as much as three times the amount of carbon (iii) compared with the surface after photoresist removed by developer (iv). The XPS spectra were normalized relative to each other. The background carbon contamination of the XPS system is less than 1 at. % meaning the detected carbon peaks originated from external carbon sources (solvents, photoresist, etc.).

energy for a reaction to occur, leading to covalently attached mdNDs to the surface (Scheme 1). The described reaction would be common to other photoresists containing novolac and particles possessing carboxylic groups on the surface. We do not expect that such a reaction can occur between hydrogen terminated nanodiamonds and the photoresist. In the case of hydrogen terminated mdNDs, it is more likely that hydrogen bonding can occur. In addition, the reader should note that if photoresists based on radical degradation are used, upon exposure to a UV light, radical chemical reaction can potentially happen between the remaining photoresist and NDs.

Nucleation of diamond outside the patterned area is unwanted for selective diamond growth. Spurious nucleation is not only undesirable because it interferes with the fabrication of high-quality patterns, but it is also problematic during a long CVD growth causing overgrowth of diamond to undesired areas. To eliminate this nucleation, the surface after the photolithography has been treated in oxygen−argon or hydrogen plasma (Figures 2a, ii−iv and 2b, ii−iv). The reason for this was to eliminate the remaining photoresist or any other source of hydrocarbon that might create a nucleation spots for diamond growth during CVD growth. However, plasma treatment has resulted in a disruption of the homogeneity of the created diamond patterns, and as a result, we saw no significant reduction in diamond autonucleation outside the pattern.

In the case of seeding with negatively charged (oxygen-treated) mdNDs on Si with utilizing a plasma cleaner, some interesting structures have been formed, where only the outline of the pattern was created (Figure 2b, iv). These linear diamond structures were formed by a single or a double layer of grown nanodiamonds (Figure SI 2 a, b, Supporting Information). The linear structures were most likely as a result of retained mdNDs along the sidewall of the photoresist due to the esterification reaction, leading to a buildup of mdNDs in the area of corner between photoresist and wafer after removal of the photoresist (Figure SI 2 c, Supporting Information). This is a novel method to pattern diamonds in a linear manner, which may find applications as patterned fluorescent markers in bio-sensing or quantum optics.

Another major factor that plays a role in diamond autonucleation is the initial surface cleanliness. Accordingly, we have examined silicon surfaces using XPS to determine the amount of the hydrocarbon that it possesses before the diamond growth (Figure 3). The high-resolution XPS analysis of carbon (C 1s) demonstrated that silicon treated in O_2/Ar plasma prior to lithography leaves the surface with a negligible amount of carbon (Figure 3, ii). A similar result has been obtained with the surface, where the photoresist was exposed to UV light followed by removal with the developer (Figure 3, iv), leading to only a small amount of the remaining photoresist. On the other hand, the surface with the photoresist removed with acetone has been left with as much as three times the amount of carbon compared with the surface after photoresist removed by developer (Figure 3, iii). The remaining carbon originated from acetone clean could lead to uncontrolled diamond nucleation in the unwanted areas.

To confirm that the residual carbon on the surface may lead to diamond nucleation, we introduced non-patterned control samples into the CVD chamber under the identical growth conditions as was used for the growth of the patterns shown in Figure 1. The control samples were clean Si, Si cleaned in O_2/Ar plasma, Si cleaned in solvents, Si after removing photoresist with acetone, Si after exposing photoresist with UV and removing it with a developer, Si with photoresist, and Si with

photoresist exposed to mdND suspension following to its removal with acetone. Subsequent to the growth, samples have been examined using SEM (Figure 4 a–d). The samples with

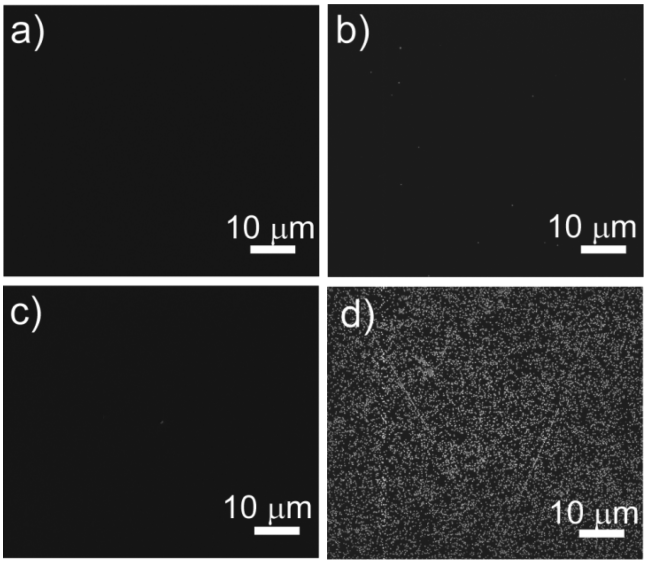

Figure 4. Representative SEM images of various silicon surfaces taken after CVD with diamond growth conditions. (a) Surface without diamond nucleation corresponds to initially clean Si surface or Si substrate cleaned in O_2/Ar plasma, or Si with photoresist removed with developer; (b) SEM image with multiple diamond nucleation sites corresponds to Si surface after the photoresist was removed with acetone and grown in the CVD; (c) SEM image with few diamond nucleation sites corresponds to Si surface with the unremoved photoresist grown in the CVD chamber; (d) SEM image of numerous nucleation results from Si with photoresist, which was immersed into mdND colloid suspension and the photoresist was removed using acetone, and diamond was grown on the patterned region in the CVD chamber. Scale bars are 10 μm.

clean Si, Si cleaned on O_2/Ar plasma, and Si after exposing photoresist with UV and removing it with a developer showed negligible nucleation of NDs on the surface as representatively demonstrated in Figure 4a. The figure is in good agreement with the data obtained from the XPS analysis. As soon as Si was exposed to acetone, low-density nucleation can be visible on the surface following the growth (Figure 4b). The presence of a photoresist layer on Si does not cause any significant diamond nucleation, as shown in Figure 4c. The most significant diamond nucleation was caused when the Si with photoresist was immersed into the mdND suspension, and subsequently, the photoresist with mdNDs was removed using acetone (Figure 4d). This suggests that dissolved photoresist with mdNDs in acetone have a secondary interaction with a Si surface, leading to a partial secondary diamond seeding of the surface and, consequently, to diamond nucleation. It is also notable that the density of the diamond seeds is higher than in the areas outside the pattern on Figure 2a, i. The increased seeding density was caused, most likely, due to a chemical reaction (esterification) between mdNDs and the remaining photoresist on the surface as described above. Overall, the remaining hydrocarbon on the surface can provide nucleation sites for diamond during the CVD growth, however the more significant nucleation occurs only when mdND seeds are attached to the surface.

Two-Step Patterning Method. To prevent the unwanted secondary seeding of mdNDs and autonucleation, we have made a use of lift-off resist (Scheme 1b). The advantage of this process is that both photoresist and lift-off resist can be exposed and developed at the same time using the same developer, but their removal requires different solvents. For instance, while the photoresist is dissolved in acetone, the lift-off resist is not acetone soluble, and can be removed only using a developer. This combination of the resists provides at least two benefits: first, secondary diamond seeding is eliminated during the removal of the lift-off resist using developer, and second, the developer is able somewhat to etch the native oxide layer,[32] providing even better cleanliness of the surface. Exposing the samples to plasma for diamond growth leads to well-defined patterns with no nucleation outside the pattern (Scheme 1b, G). The dark area on the image is an artifact due to charging occurring during image acquisition (Figure SI 3a, Supporting Information). Furthermore, only seeding with positively-charged mdND suspensions leads to a clear pattern with high-density diamond nucleation, whereas negatively-charged mdNDs have no interaction with the surface, resulting in no patterns (Figure SI 3b, Supporting Information).

Once the process had been established on Si, we translated the two step lithography patterning approach to the other surfaces (AlN and sapphire). Figure 5 shows the pattern formation on the two substrates, AlN (a, b) and sapphire (c, d), using two-step lithography and seeding protocols. When AlN was seeded with negatively-charged diamond colloids, there was

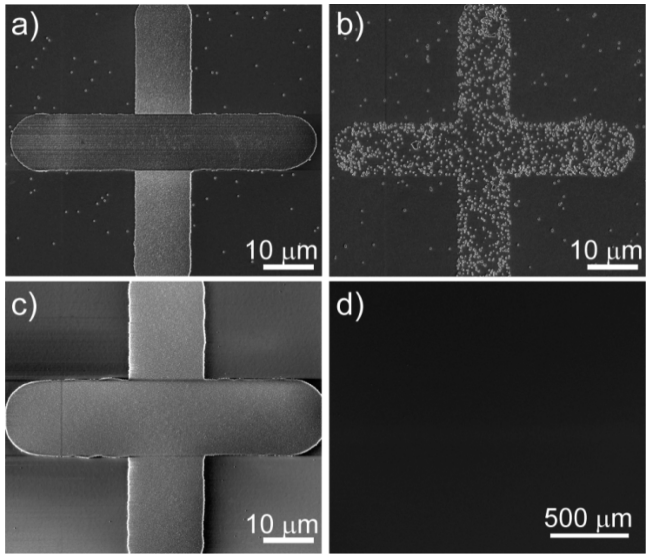

Figure 5. SEM images of the diamond patterns on AlN (a, b) and sapphire (c, d) fabricated using the two step photolithography patterning method and mdNDs seeding with negatively charged (a, c) and positively charged (b, d) mdNDs. When AlN and sapphire were seeded with negatively charged diamond colloids, there was a formation of highly dense diamond pattern with nucleation density as high as 10^{11} cm^{-2}. When positively charged colloids have been used in the seeding process, no pattern was formed on the surface of sapphire, while on AlN there is still a low density pattern visible. The C-plane of sapphire is highly positively charged (~60 mV) providing an efficient electrostatic repulsion to positively charged mdNDs. On the other hand, AlN is less charged than sapphire as nitrogen content contributes to ammonia production, bringing pH to more neutral, and consequently allowing the attraction of mdNDs to the surface through hydrogen or van der Waals forces.

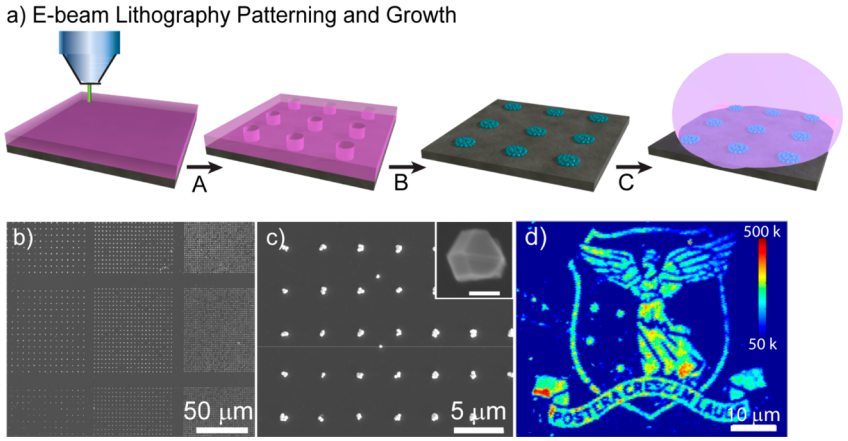

Figure 6. (a) Schematic representation of the combination of e-beam lithography and seeding with colloid mdNDs on silicon substrate: PMMA is spun on the substrate and cured, and then the pattern is written onto PMMA using electron beam (A), developed using MIBK and seeded in the negatively charged mdND colloid suspensions. PMMA with unwanted NDs is removed with acetone (B), and the substrate with mdNDs on it introduced to diamond growth conditions in CVD chamber (C); (b) SEM image of ND seeds were grown in the patterned manner using rastering the e-beam; (c) high-resolution pattern of ND seeds grown in controlled manner with equal distances. The inset shows that technique can allow individual single crystals diamonds to be grown at a desired location (scale bar is 100 nm); (d) confocal laser scanning microscopy image of logo of the University of Melbourne patterned and fabricated using e-beam lithography and seeding with colloid mdNDs after CVD growth. The fluorescence originates from the Si-vacancy diamond color centers. Color scale represents the fluorescence intensity from 50 to 500 Kcounts·s^{-1}.

a formation of highly dense diamond pattern with a nucleation density as high as 10^{11} seeds per cm^2 (Figure 5a). Such a high nucleation density occurs because of electrostatic interaction between AlN and oxygen treated mdNDs. AlN exhibits a positively charge in an aqueous environment due to its oxide layer, which hydrolyses into AlO(OH) or $Al(OH)_3$ in water.[33] Al−OH groups on the surface of AlN act as proton acceptors, leading to a positive zeta potential on the surface. Similarly, we formed patterns on the surface of sapphire using oxygen treated mdND colloids (Figure 5c). C-plane sapphire surface consists of aluminum oxide that hydrolyses in acidic water (pH below 4) to produce $-Al(OH_2^+)$, which exhibits a positive zeta potential in water.[34,35] When positively charged colloids have been used in the seeding process, no pattern was formed on the surface of sapphire (Figure 5d), whereas on AlN, there is still a low density pattern visible (Figure 5b). The C-plane of sapphire is highly positively charged (~60 mV), providing an efficient electrostatic repulsion to positively charged mdNDs. On the other hand, AlN is less charged than sapphire as nitrogen content contributes to ammonia production, making the pH more neutral, and consequently allowing the attraction of mdNDs to the surface through hydrogen or van der Waals forces.

Submicrometer Patterning Method. Described above is the method to create diamond patterns with micrometer resolution. To achieve a submicrometer resolution, we utilized e-beam lithography at 30 keV using PMMA as a resist and MIBK:IPA (1:3) as a developer for the fabrication of high-resolution patterns. The patterns were produced using a single resist (PMMA) approach (Figure 6a), but the use of lift-off resist is also compatible with the e-beam lithography that potentially can produce cleaner diamond patterns. The patterns of holes in PMMA were produced using two methods: by rastering the e-beam and by exposing a single point. The holes patterned in the resist by rastering the beam are much better defined than those created by exposing a single point (Figure SI 4, Supporting Information). The developed high-resolution patterns on Si were seeded in the oxygen-treated mdND suspension and inserted into a CVD chamber for diamond growth (Figure 6a). Hydrogen treated mdNDs were not found to be attracted to these patterns (not shown). XPS analysis of a PMMA film, before and after development reveals that the PMMA was overexposed. This results in a monolayer of PMMA, which cannot be removed by the developer (Figure SI 5, Supporting Information), and appears to be critical in attracting the oxygen terminated mdNDs. Yet, the use of overexposure may limit the ultimate lateral resolution of the e-beam lithography technique. Figure 6b shows CVD grown patterned arrays of diamond particles on the surface of silicon. By varying hole diameter and pitch in the patterns, we have achieved the fabrication of ND crystal arrays (Figure 6b). In addition, the amount of diamond can be controlled by the size of the fabricated hole, where Figure 6b demonstrates that the average number of diamond crystals grown in each hole with the diameter of 300 nm is 3.6 ± 1.5. There is thus a possibility to grow even a single diamond nanocrystal in each location (Figure 6c, inset). Although the e-beam lithography employed has only hundred-nanometer resolution, it is possible to achieve single nanodiamond crystal positioning and growth by using a lower ND seeding density, such as 5×10^{-9} seeds/cm^2. This high resolution technique is particularly useful for fabrication of fluorescent nanodiamond arrays containing different optical centers, such as NV centers, which hold great promise in quantum photonics and sensing applications.[11,36] For example, we have fabricated a logo of the University of Melbourne using e-beam lithography and colloid mdND seeding on Si followed by CVD growth (Figure 6d). Imaging of the pattern using confocal microscopy reveals fluorescence originating from Si-vacancy color centers within the diamond lattice (Figure 6d).

CONCLUSION

We have developed a robust approach to patterning diamond thin films on various substrates, such as silicon, AlN, and sapphire. Photo- and e-beam lithography and mdND colloid seeding protocols were used. We identified various factors that affect the selective seeding on different substrates, such as mdND surface termination, zeta potential, surface treatment, and plasma cleaning. We have shown that although the

electrostatic interaction between mdND colloids and substrates is the main driving force, there are scenarios where chemical reaction (esterification) or hydrogen bonding occur and dominate the mdND seeding process. Our patterning recipes allow elimination of unwanted diamond nucleation outside the patterned areas that are detrimental to a fabrication of high quality patterns. In addition, by combination of photolithography, mdND seeding, and plasma etching, we have revealed a novel way to fabricate single linear patterns of diamonds. More importantly, we have demonstrated the fabrication of high resolution diamond patterns using the combination of e-beam lithography and the mdND seeding procedures. In particular, we have achieved the deposition of single diamond seeds in patterned manner over a range of feature sizes. This provides a useful technique to selectively grow single ND particles on a range of substrates. Overall, this study contributes to a comprehensive understanding of the mdND and substrate interaction and reveals the important factors influencing high-resolution ND patterning.

■ ASSOCIATED CONTENT

Supporting Information

FTIR spectra of different ND powders; high resolution SEM images of diamond pattern formed using negatively-charged mdNDs (annealed in oxygen) colloids on Si, where hydrogen plasma was applied prior to diamond growth; high magnification SEM image of diamond pattern of Si formed through the double photoresist layer patterning approach, where positively charged mdND colloids were used and low magnification SEM image of diamond pattern on Si formed through the enhanced patterning approach, where the negatively charged mdND colloids were used; SEM image of ND seeds grown in the patterned manner using single point exposure and higher magnification of one of the diamond pattern elements; XPS spectra of the C 1s peak originated from PMMA and PMMA after e-beam exposure and development procedure. This material is available free of charge via the Internet at http://pubs.acs.org.

■ AUTHOR INFORMATION

Corresponding Author

* Dr. Olga Shimoni. E-mail: Olga.Shimoni@uts.edu.au.

Present Addresses

[§]School of Physics and Advanced Materials, University of Technology, Sydney (UTS), Broadway, NSW 2007, Australia
[⊥]On leave from Institute of Physics ASCR, v. v. i., Cukrovarnicka 10, Prague, Czech Republic.

Author Contributions

The paper was written through contributions of all authors. All authors have given approval to the final version of the paper.

Funding

This research was supported by the Australian Research Council Projects (LP0991781, LP 100100524 and DP 1096288). B.C.G. is supported by an ARC Future Fellowship (FT110100225).

Notes

The authors declare no competing financial interest.

■ ACKNOWLEDGMENTS

The authors acknowledge the technical assistance of Marta Redrado Notivoli, Chemical and Biomolecular Engineering Department, Dr. Desmond Lau and Dr. Kumaravelu Ganesan at School of Physics for useful discussions. Nikolai Dontschuk is gratefully acknowledged for the initial development of mdND suspension protocols. The authors acknowledge the Electron Microscopy unit of Bio21 Institute, The University of Melbourne, for assistance with electron microscopy. The authors acknowledge the facilities, and the scientific and technical assistance, of the Australian Microscopy & Microanalysis Research Facility at the RMIT Microscopy & Microanalysis Facility, at RMIT University.

■ ABBREVIATIONS

AlN = aluminum nitride
CVD = chemical vapor deposition
DI = deionized water
FTIR = Fourier transform infrared spectroscopy
IPA = isopropyl alcohol
KBr = potassium bromide
ND = nanodiamond
MIBK = methyl isobutyl ketone
mdND = monodispersed nanodiamond
NCD = nanocrystalline diamond
PMMA = poly(methyl methacrylate)
SEM = scanning electron microscopy
UV = ultraviolet
XPS = X-ray photoelectron spectroscopy

■ REFERENCES

(1) Williams, O. A.; Nesládek, M. Growth and Properties of Nanocrystalline Diamond Films. *Phys. Status Solidi A* **2006**, *203*, 3375−3386.
(2) Shen, Z. H.; Hess, P.; Huang, J. P.; Lin, Y. C.; Chen, K. H.; Chen, L. C.; Lin, S. T. Mechanical Properties of Nanocrystalline Diamond Films. *J. Appl. Phys.* **2006**, *99*, 124302.
(3) Sharda, T.; Soga, T.; Jimbo, T. Optical Properties of Nanocrystalline Diamond Films by Prism Coupling Technique. *J. Appl. Phys.* **2003**, *93*, 101−105.
(4) Krauss, A. R.; Auciello, O.; Gruen, D. M.; Jayatissa, A.; Sumant, A.; Tucek, J.; Mancini, D. C.; Moldovan, N.; Erdemir, A.; Ersoy, D.; Gardos, M. N.; Busmann, H. G.; Meyer, E. M.; Ding, M. Q. Ultrananocrystalline Diamond Thin Films for MEMS and Moving Mechanical Assembly Devices. *Diamond Relat. Mater.* **2001**, *10*, 1952−1961.
(5) Hees, J.; Heidrich, N.; Pletschen, W.; Sah, R. E.; Wolfer, M.; Williams, O. A.; Lebedev, V.; Nebel, C. E.; Ambacher, O. Piezoelectric Actuated Micro-Resonators Based on the Growth of Diamond on Aluminum Nitride Thin Films. *Nanotechnology* **2013**, *24*, 025601.
(6) Philip, J.; Hess, P.; Feygelson, T.; Butler, J. E.; Chattopadhyay, S.; Chen, K. H.; Chen, L. C. Elastic, Mechanical, and Thermal Properties of Nanocrystalline Diamond Films. *J. Appl. Phys.* **2003**, *93*, 2164−2171.
(7) Hutchinson, A. B.; Truitt, P. A.; Schwab, K. C.; Sekaric, L.; Parpia, J. M.; Craighead, H. G.; Butler, J. E. Dissipation in Nanocrystalline Diamond Nanomechanical Resonators. *Appl. Phys. Lett.* **2004**, *84*, 972−974.
(8) Verhoeven, H.; Boettger, E.; Flöter, A.; Reiß, H.; Zachai, R. Thermal Resistance and Electrical Insulation of Thin Low-Temperature-Deposited Diamond Films. *Diamond Relat. Mater.* **1997**, *6*, 298−302.
(9) Grausova, L.; Kromka, A.; Bacakova, L.; Potocky, S.; Vanecek, M.; Lisa, V. Bone and Vascular Endothelial Cells in Cultures on Nanocrystalline Diamond Films. *Diamond Relat. Mater.* **2008**, *17*, 1405−1409.
(10) Chen, Y.-C.; Lee, D.-C.; Hsiao, C.-Y.; Chung, Y.-F.; Chen, H.-C.; Thomas, J. P.; Pong, W.-F.; Tai, N.-H.; Lin, I. N.; Chiu, I.-M. Bone and Vascular Endothelial Cells in Cultures on Nanocrystalline Diamond Films. *Biomaterials* **2009**, *30*, 3428−3435.

(11) Aharonovich, I.; Greentree, A. D.; Prawer, S. Diamond photonics. *Nat. Photonics* **2011**, *5*, 397−405.
(12) Aharonovich, I.; Castelletto, S.; Simpson, D.; Su, S.-H.; Greentree, A. D.; Prawer, S. Diamond-Based Single-Photon Emitters. *Rep. Prog. Phys.* **2011**, *74*, 076501.
(13) Akhvlediani, R.; Lior, I.; Michaelson, S.; Hoffman, A. Nanometer Rough, Sub-Micrometer Thick and Continuous Diamond Chemical Vapor Deposition Film Promoted by a Synergetic Ultrasonic Effect. *Diamond Relat. Mater.* **2002**, *11*, 545−549.
(14) Iijima, S.; Aikawa, Y.; Baba, K. Early Formation of Chemical Vapor Deposition Diamond Films. *Appl. Phys. Lett.* **1990**, *57*, 2646−2648.
(15) Daenen, M.; Williams, O. A.; D'Haen, J.; Haenen, K.; Nesládek, M. Seeding, Growth and Characterization of Nanocrystalline Diamond Films on Various Substrates. *Phys. Status Solidi A* **2006**, *203*, 3005−3010.
(16) Williams, O. A.; Douheret, O.; Daenen, M.; Haenen, K.; Osawa, E.; Takahashi, M. Enhanced Diamond Nucleation on Monodispersed Nanocrystalline Diamond. *Chem. Phys. Lett.* **2007**, *445*, 255−258.
(17) Hees, J.; Kriele, A.; Williams, O. A. Electrostatic Self-Assembly of Diamond Nanoparticles. *Chem. Phys. Lett.* **2011**, *509*, 12−15.
(18) Seung-Koo, L.; Jong-Hoon, K.; Min-Goon, J.; Min-Jung, S.; Dae-Soon, L. Direct Deposition of Patterned Nanocrystalline CVD Diamond Using an Electrostatic Self-Assembly Method with Nanodiamond Particles. *Nanotechnology* **2010**, *21*, 505302.
(19) Wang, X. P.; Ocola, L. E.; Divan, R. S.; Sumant, A. V. Nanopatterning of Ultrananocrystalline Diamond Nanowires. *Nanotechnology* **2012**, *23*, 075301.
(20) Narayan, J.; Chen, X. Laser Patterning of Diamond Films. *J. Appl. Phys.* **1992**, *71*, 3795−3801.
(21) Santori, C.; Barclay, P. E.; Fu, K.-M. C.; Beausoleil, R. G. Vertical Distribution of Nitrogen-Vacancy Centers in Diamond Formed by Ion Implantation and Annealing. *Phys.Rev. B* **2009**, *79*, 125313.
(22) Gaebel, T.; Domhan, T. M.; Wittmann, C.; Popa, I.; Jelezko, F.; Rabeau, J.; Greentree, A. D.; Prawer, S.; Trajkov, E.; Hemmer, P. R.; Wrachtrup, J. Photochromism in Single Nitrogen-Vacancy Defect in Diamond. *Appl. Phys. B* **2006**, *82*, 243−246.
(23) Williams, O. A.; Hees, J.; Dieker, C.; Jager, W.; Kirste, L.; Nebel, C. E. Size-Dependent Reactivity of Diamond Nanoparticles. *ACS Nano* **2010**, *4*, 4824−4830.
(24) Cervenka, J.; Lau, D. W. M.; Dontschuk, N.; Shimoni, O.; Silvestri, L.; Ladouceur, F.; Duvall, S. G.; Prawer, S. Nucleation and Chemical Vapor Deposition Growth of Polycrystalline Diamond on Aluminum Nitride: Role of Surface Termination and Polarity. *Cryst. Growth Des.* **2013**, *13*, 3490−3497.
(25) Aharonovich, I.; Zhou, C.; Stacey, A.; Treussart, F.; Roch, J.-F.; Prawer, S. Formation of Color Centers in Nanodiamonds by Plasma Assisted Diffusion of Impurities From the Growth Substrate. *Appl. Phys. Lett.* **2008**, *93*, 243112.
(26) Mochalin, V. N.; Shenderova, O.; Ho, D.; Gogotsi, Y. The Properties and Applications of Nanodiamonds. *Nat. Nanotechnol.* **2012**, *7*, 11−23.
(27) Chakrapani, V.; Angus, J. C.; Anderson, A. B.; Wolter, S. D.; Stoner, B. R.; Sumanasekera, G. U. Charge Transfer Equilibria Between Diamond and an Aqueous Oxygen Electrochemical Redox Couple. *Science* **2007**, *318*, 1424−1430.
(28) Girard, H. A.; Petit, T.; Perruchas, S.; Gacoin, T.; Gesset, C.; Arnault, J. C.; Bergonzo, P. Surface Properties of Hydrogenated Nanodiamonds: a Chemical Investigation. *Phys. Chem. Chem. Phys.* **2011**, *13*, 11517−11523.
(29) Pobedinskas, P.; Degutis, G.; Dexters, W.; Janssen, W.; Janssens, S. D.; Conings, B.; Ruttens, B.; D'Haen, J.; Boyen, H.-G.; Hardy, A.; Van Bael, M. K.; Haenen, K. Surface Plasma Pretreatment for Enhanced Diamond Nucleation on AlN. *Appl. Phys. Lett.* **2013**, *102*, 201609.
(30) Girard, H. A.; Arnault, J. C.; Perruchas, S.; Saada, S.; Gacoin, T.; Boilot, J. P.; Bergonzo, P. Hydrogenation of Nanodiamonds Using MPCVD: A New Route Toward Organic Functionalization. *Diamond Relat. Mater.* **2010**, *19*, 1117−1123.
(31) Chu, C. D.; Perevedentseva, E.; Yeh, V.; Cai, S. J.; Tu, J. S.; Cheng, C. L. Temperature-Dependent Surface CO Stretching Frequency Investigations of Functionalized Nanodiamond Particles. *Diamond Relat. Mater.* **2009**, *18*, 76−81.
(32) Thong, J. T. L.; Choi, W. K.; Chong, C. W. TMAH Etching of Silicon and the Interaction of Etching Parameters. *Sens. Actuators, A* **1997**, *63*, 243−249.
(33) Graziani, T.; Bellosi, A. Degradation of Dense AlN Materials in Aqueous Environments. *Mater. Chem. Phys.* **1993**, *35*, 43−48.
(34) Franks, G. V.; Meagher, L. The Isoelectric Points of Sapphire Crystals and Alpha-Alumina Powder. *Colloids Surf., A* **2003**, *214*, 99−110.
(35) Kershner, R. J.; Bullard, J. W.; Cima, M. J. Zeta Potential Orientation Dependence of Sapphire Substrates. *Langmuir* **2004**, *20*, 4101−4108.
(36) McGuinness, L. P.; Yan, Y.; Stacey, A.; Simpson, D. A.; Hall, L. T.; Maclaurin, D.; Prawer, S.; Mulvaney, P.; Wrachtrup, J.; Caruso, F.; Scholten, R. E.; Hollenberg, L. C. L. Quantum Measurement and Orientation Tracking of Fluorescent Nanodiamonds Inside Living Cells. *Nat. Nanotechnol.* **2011**, *6*, 358−363.